

## Simulation of Three-Dimensional Flow Field around Unconventional Bridge Piers

Adnan Ismael<sup>1</sup> & Hamid Hussein<sup>2</sup> & Mohammed Tareq<sup>3</sup> & Mustafa Gunal<sup>4</sup>

<sup>1</sup>Technical Institute, Mosul, Iraq

<sup>2</sup>Technical College, Mosul, Iraq

<sup>3</sup>Civil engineering, Ishik University, Erbil, Iraq

<sup>4</sup>Civil Engineering, Gaziantep University, Turkey

Correspondence: Adnan Ismael, Technical Institute, Mosul, Iraq. Email: adnan\_esmaeel@yahoo.com

Received: August 21, 2017    Accepted: November 3, 2017    Online Published: December 1, 2017

doi: 10.23918/eajse.v3i2p90

**Abstract:** The study presents a three-dimensional numerical simulation of turbulent flow field around unconventional bridge piers which are downstream-facing round-nosed (DS-FRNP) and upstream-facing round-nosed (US-FRNP) and are compared with a circular pier in fixed-bed using the computational fluid dynamics (CFD). In this paper, the flow field passing around the bridge piers is predicted using  $k-\omega$  standard turbulence model. The predicted flow velocity in x-direction and turbulent kinetic energy (TKE) are compared with the tested data. Simulated flow velocity and turbulent kinetic energy are in good agreement with experimental data. Numerical model predicts the flow features such as flow reversal upstream the pier, down flow upstream the pier and flow in wake region, the shape of vortices (horse shoe vortex and wake vortex) also captured by simulation. The discussion of the relation between bridge pier shape and turbulent kinetic energy in this study will help to control the scour around bridge piers.

**Keywords:** CFD,  $K-\omega$  Model, 3D Turbulence Flow And Unconventional Bridge Pier

### 1. Introduction

Local scour around bridge pier is the leading cause of bridge failure, effecting significantly on the total construction and maintenance costs. Therefore, scouring around uniform pier with cylindrical shape is commonly used in the field. The shape of bridge piers has important effect on the local scour. A literature review showed that there is still a lack of experimental studies on the effects of non-uniform pier. The flow around a pier is three-dimensional and turbulent. CFD models have become suitable tool to predict and analysis flow for different river engineering problems. However, their applicability has to be proven using experimental data or field measurements. For flow around bridge pier in a fixed-bed, the existence of vortices from the bridge pier initiates a scour hole. This local scour may lead to failure of bridge pier.

Several experimental and numerical have been conducted to investigate the 3D flow and turbulence around piers in a fixed-bed. Graf and Istiarto (2002) detected velocities, turbulence intensities, Reynolds stresses, and bed-shear stresses in different azimuthal planes within the equilibrium scour hole at a circular pier by using Acoustic Doppler Velocity Profiler (ADVP). Nagata et al. (2005) performed a model based on the Reynolds Averaged Navier Stokes equations, together with the  $k-$

epsilon turbulence model for bed deformation around bridge pier. Afzal (2013) performed two turbulence models ( $k - \omega$  and  $k - \epsilon$ ) to simulate a complex sediment transport using CFD around abutment and pier. The numerical results have been validated with physical experiment. Comparison in performance of ( $k - \omega$  and  $k - \epsilon$ ) turbulence models is done for abutment and pier scour under constant discharge. The result reveals that the performance of the  $k - \omega$  model is similar to the  $k - \epsilon$  in the pier scour case. Guemou et al. (2013) performed DES to simulate the flow around two bridge piers (circular and round-nosed pier) fixed in flat-bed. The authors chose the DES turbulence model for his ability to capture the dynamics of the horseshoe vortex, at the upstream of pier. Mammari and Soudani (2012) numerically tested the flow field around a cylinder on a fixed-bed open channel using CFD code to analysis the flow field and kinetic energy field around the pier with the standard  $k - \epsilon$  turbulence model. The predicted velocity and turbulent kinetic energy were compared with those of measured data. Roulund et al. (2005) calculated the flow and scouring around a cylindrical pile, using a model that uses the rigid- bed. Tseng et al. (2000) simulated numerically the three dimensional turbulent flow fields around circular and square piers. The results showed that the down flow strength and the domain of the high bed shear stress were greater in the case of square pier.

The objective of the present study is predicting the flow field and turbulent kinetic energy around bridge piers using CFD,  $k - \omega$  standard turbulent model. The prediction will use the same hydraulic condition as in laboratory experiments; this permits a direct comparison between the simulation and experimental data.

### 1.1 Geometric Setup

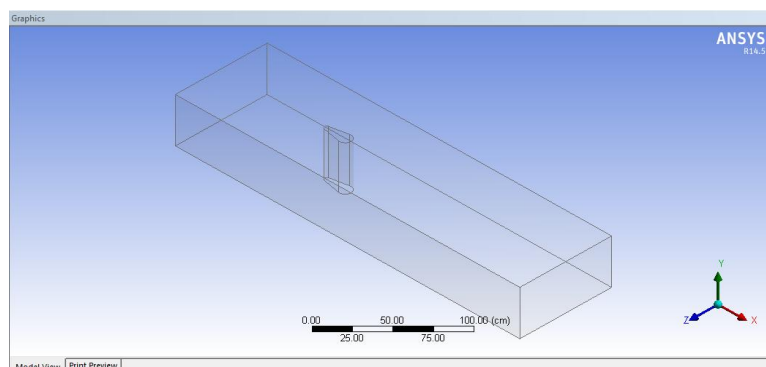


Figure 1: The geometric setup for the numerical simulation

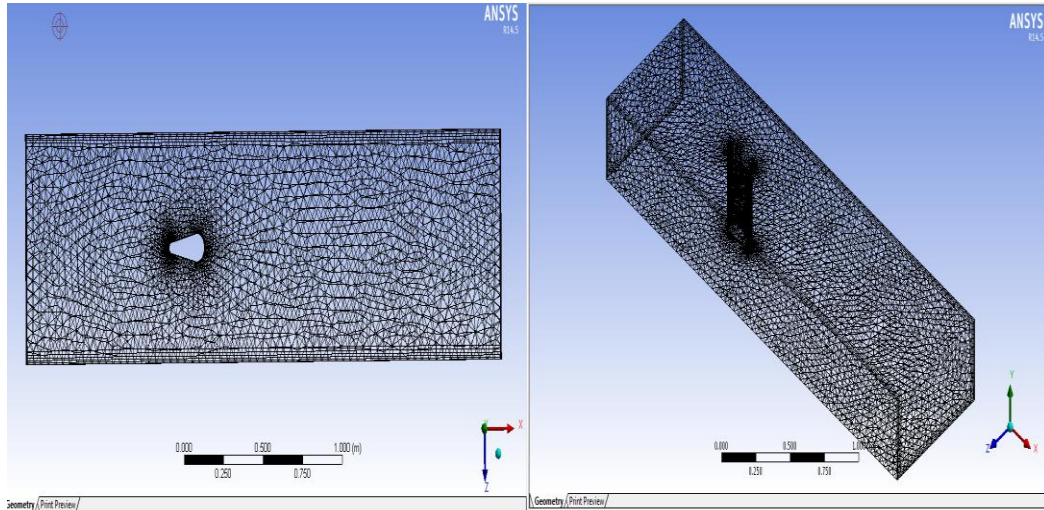


Figure 2: Mesh refinement around bridge pier

Figures 1 and 2 show location of the pier and the mesh around the pier.

## 1.2 Numerical Simulation

$k-\omega$  consist of two transported variable 1. is turbulent kinetic energy  $k$ . 2. is the specific turbulent dissipation using  $\omega$ . The turbulent eddy viscosity  $\nu_t$  is calculated using  $k$  and  $\omega$ . Using average and a fluctuating components in the Navier-Stokes equation (equation1), yields after averaging of the equations, the Reynolds equation as in equation 2 below.

$$\frac{\partial U_i}{\partial t} + U_j \frac{\partial U_i}{\partial x_j} = -\frac{1}{\rho} \frac{\partial P}{\partial x_i} + \frac{\partial}{\partial x_j} \left[ \nu \left( \frac{\partial U_i}{\partial x_j} + \frac{\partial U_j}{\partial x_i} \right) \right] + g_i \quad (1)$$

$$\frac{\partial U_i}{\partial t} + U_j \frac{\partial U_i}{\partial x_j} = -\frac{1}{\rho} \frac{\partial P}{\partial x_i} + \frac{\partial}{\partial x_j} \left[ (\nu + \nu_t) \left( \frac{\partial U_i}{\partial x_j} + \frac{\partial U_j}{\partial x_i} \right) \right] + g_i \quad (2)$$

The equations for turbulent kinetic energy  $k$  and the specific turbulent dissipation is as follows:

$$\frac{\partial k}{\partial t} + U_j \frac{\partial k}{\partial x_j} = \frac{\partial}{\partial x_j} \left[ \left( \nu + \frac{\nu_t}{\sigma_k} \right) \frac{\partial k}{\partial x_j} \right] + P_k - \beta_k k \omega \quad (3)$$

$$\frac{\partial \omega}{\partial t} + U_j \frac{\partial \omega}{\partial x_j} = \frac{\partial}{\partial x_j} \left[ \left( \nu + \frac{\nu_t}{\sigma_\omega} \right) \frac{\partial \omega}{\partial x_j} \right] + \frac{\omega}{k} \alpha P_k - \beta_\omega \omega^2 \quad (4)$$

$P_k$  is the turbulent production rate given by equation (5), the coefficients in equation 3 and 4 have the values  $\alpha = \frac{5}{9}$ ,  $\beta_k = \frac{9}{100}$  and  $\beta = \frac{3}{40}$ .

$$P_k = \nu_t \frac{\partial U_i}{\partial x_j} \left( \frac{\partial U_i}{\partial x_j} + \frac{\partial U_j}{\partial x_i} \right) \quad (5)$$

The eddy viscosity  $\nu_t$  in the RANS-equations is obtained using the two-equation  $k-\omega$  model Wilcox

(1994).

$$v_t = \min \left( \frac{k}{\omega} \sqrt{\frac{2}{3} \frac{k}{|S|}} \right) \quad (6)$$

## 2. Experiments

The experiments for validation purpose were conducted in the Hydraulics Laboratory of Gaziantep University in a rectangular channel 120 cm long, 80 cm wide and 89 cm deep. Unconventional and circular piers were used as shown in Figure 3.

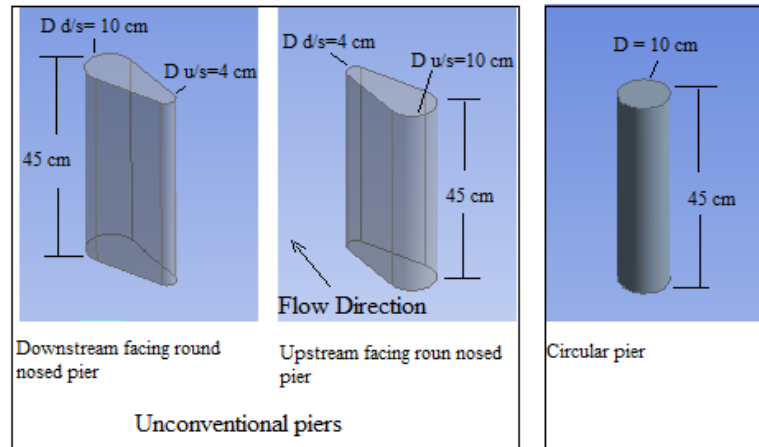


Figure 3: Dimension of unconventional and circular bridge piers

## 3. Result And Discussion

In Figure 4, velocity vectors in the vertical cross section along the channel centerline are plotted. Upstream face of (US-FRNP), the flow has more or less uniform velocity profiles, with no sign to the vertical velocities. Close to bridge pier, the vertical velocity is downward and the longitudinal velocity decreases with decreasing distance to the pier and exhibit negative values meaning that the flow reversal direction happens. At the end of the pier, the vertical velocities are downward while the longitudinal velocities exhibit negative values in the vicinity of the pier.

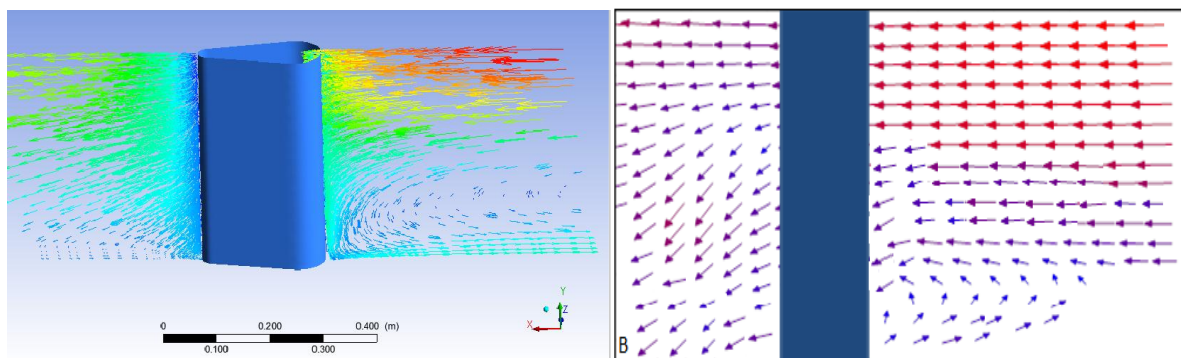


Figure 4: (a) Predicted velocity vectors and (b) Measured velocity vectors at a vertical cross section along the centerline of the model channel.

Vortices features are well captured in the front and behind of normal bridge pier. In spite of the model applied in this simulation is not expected to capture details of the features. Figure 5 shows

some interesting patterns upstream and downstream of the pier. The three dimension feature of the horseshoe vortex clockwise extends toward downstream.

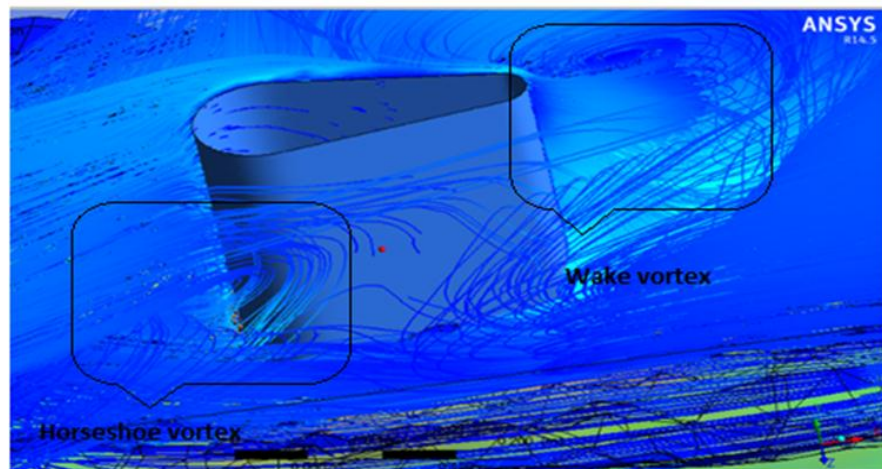


Figure 5: Vortices upstream and downstream bridge pier

In Figure 6, volume rendering of (TKE) in the plane  $z = 0.25H$  above the bed are plotted for three bridge piers. The maximum value of TKE for (DS-FRNP) is  $(0.002425 \text{ J/kg})$  reduced as compared to (US-FRNP)  $(0.0679 \text{ J/kg})$  and circular  $(0.06944 \text{ J/kg})$  piers. That means the magnitude of vorticity is more reduced in case of (DS-FRNP), which results in reduced local scour.

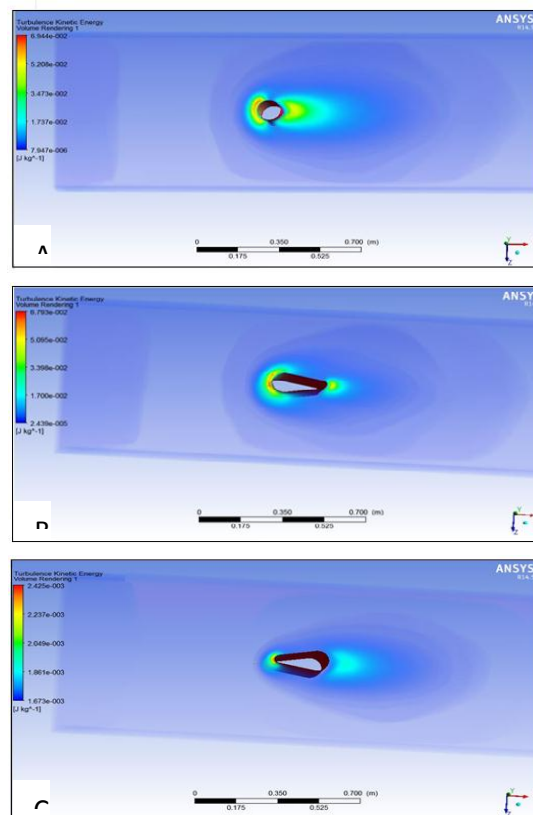


Figure 6: Volume rendering of TKE ( $\text{J kg}^{-1}$ ) for A) Circular, B) (US-FRNP) and C) (DFRNP)

Figure 7 shows flow separation as the flow passes around the three bridge piers, flow separation produces wake vortex behind the bridge piers. Maximum velocities for circular and (US-FRNP) are observed about  $75^\circ$  by Oliveto and Hager (2002).

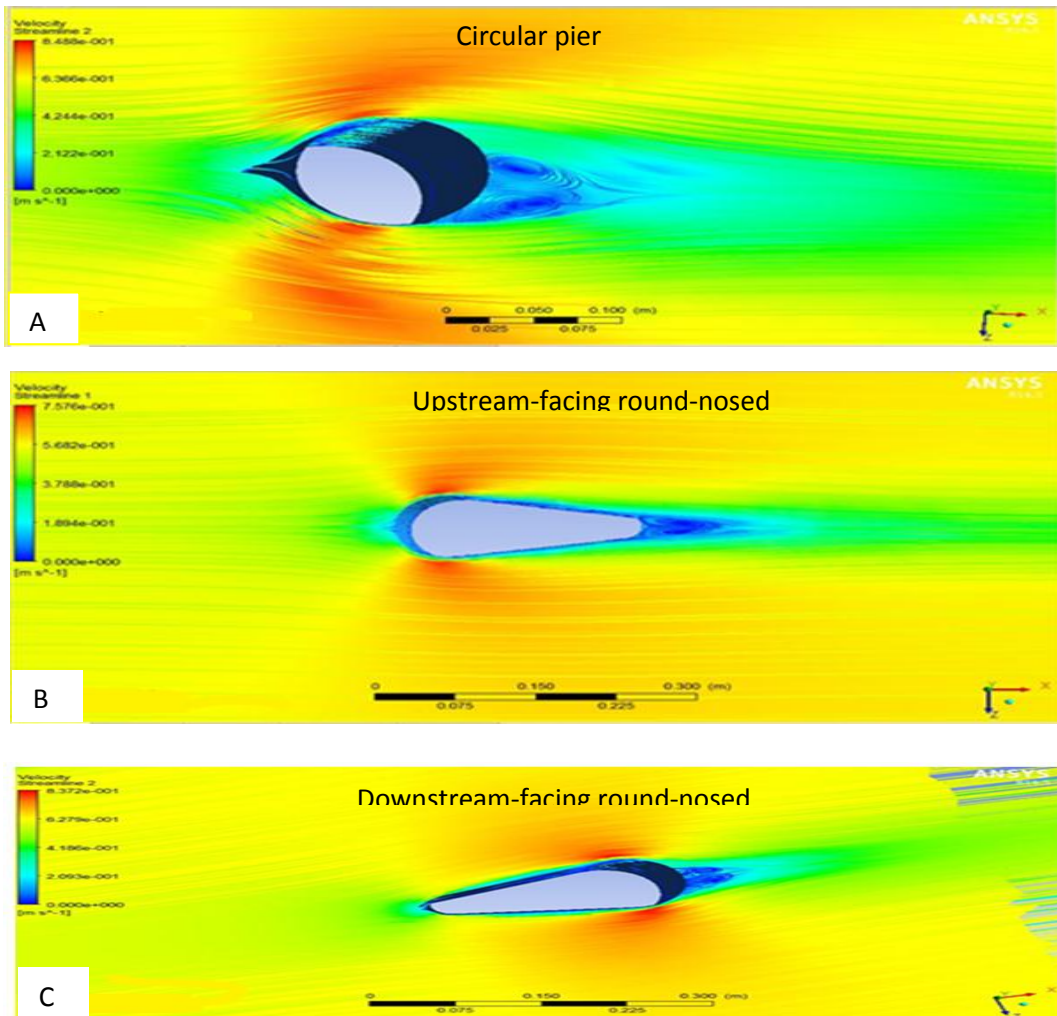


Figure 7: Streamlines shows flow separations around A) Circular, B) (US-FRNP) and C) (DS-FRNP)

Figures (8-9) show a comparison between predicted and measured velocities and turbulent kinetic energy respectively upstream face of the bridge piers. For standard  $k-\omega$  model the correlation coefficient shows a good agreement for longitudinal velocity ( $v_u$ ) and (TKE) with  $R^2$  (0.898) and  $R^2$  (0.96) respectively.

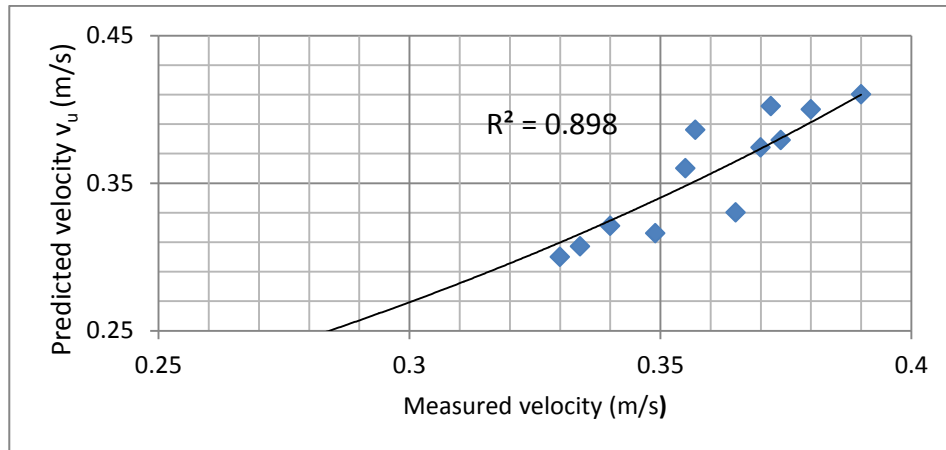


Figure 8: A comparison between predicted and measured velocities at upstream face of piers located along the centerline of the models channel

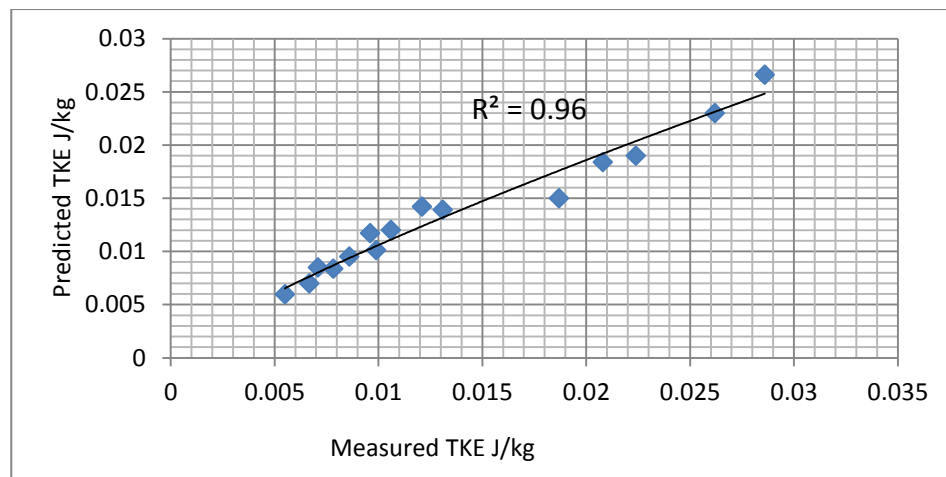


Figure 9: A comparison between predicted and measured TKE at upstream face of piers located along the centerline of the models channel

#### 4. Validation of Results

The standard ( $k-\omega$ ) model has been then applied to simulate the case of flow around (DS-FRNP), (US-FRNP) and circular piers in a channel with a fixed bed. The experimental data were compared with the results of CFD. Figure 10 (A,B and C) shows the longitudinal velocity upstream three piers, we notice that longitudinal velocity increases as far as from piers, but decreases when approaching the piers. For the turbulent kinetic energy as shown in Figure 11 (A,B and C), there is a good agreement between the simulated and experimental results. Maximum TKE observed close to pier then decreased a way from the pier.

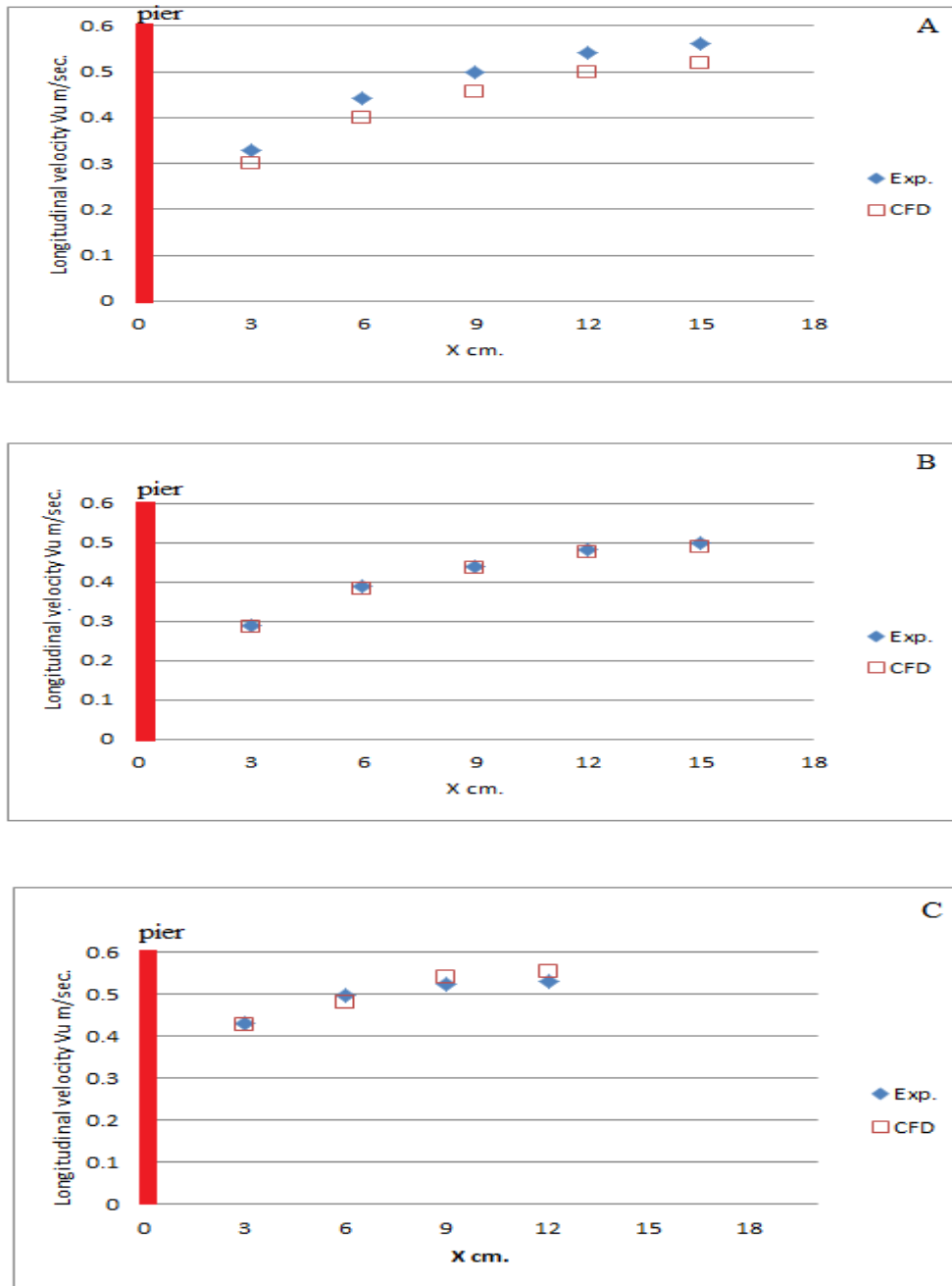


Figure 10: Longitudinal velocity upstream A) Circular pier, B) (US-FRNP) and C) (DS-FRNP)

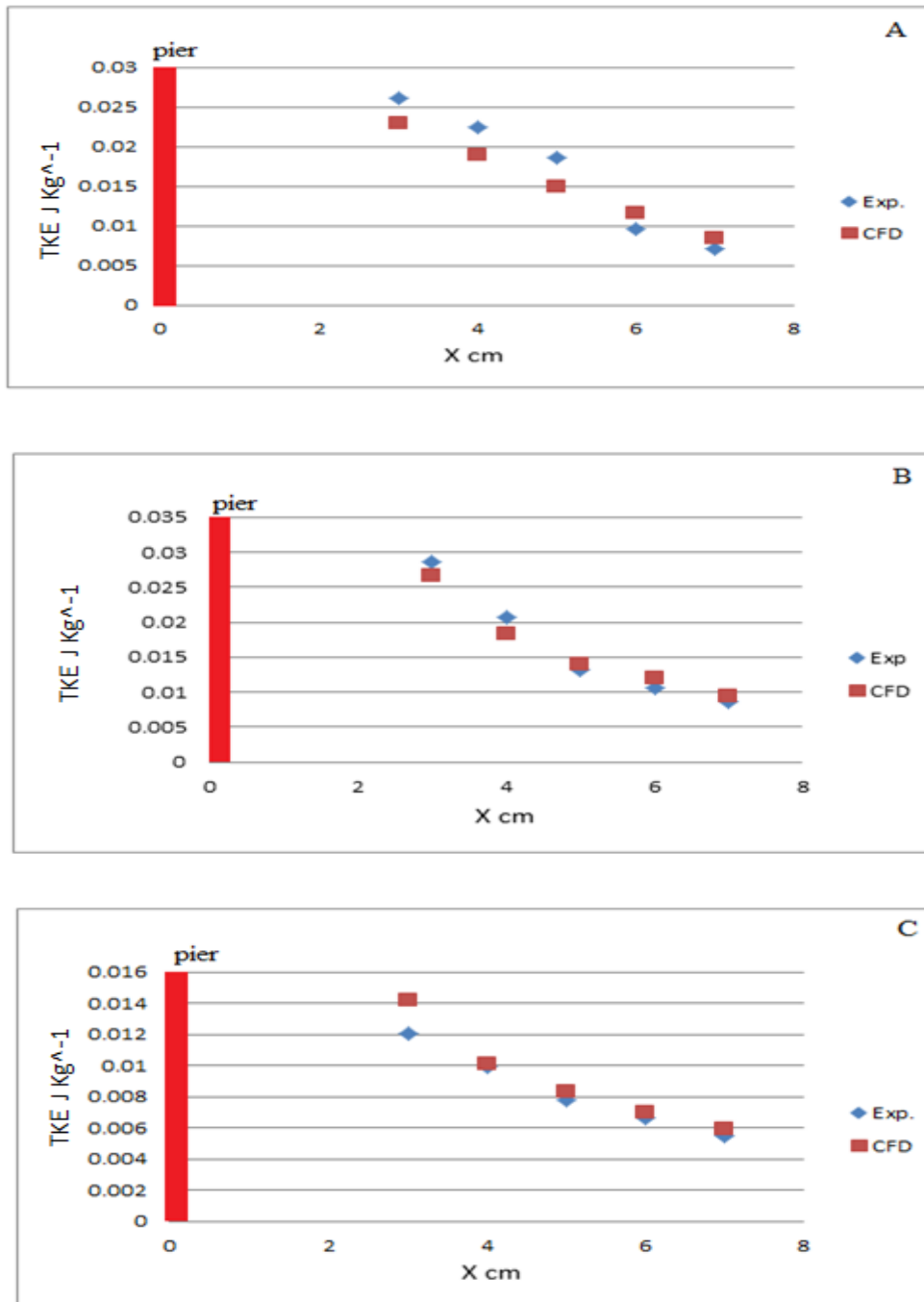


Figure 11: TKE values with distance near A) Circular pier, B (US-FRNP) and C) (DS-FRNP)

## 5. Conclusion

CFD simulation shows the ability of k-omega turbulent model to capture the features of the complicate 3D flow field (flow velocity, turbulent kinetic energy and vortices in wake region of the pier) around the bridge pier. Predictions of the flow field and the TKE are well correlated with experimental data, with a correlation coefficient of 0.898 and 0.96 respectively. Other features

predicted include the horseshoe vortex and wake vortex. For model validation the experimental data was chosen for the bridge piers. The following conclusions could be drawn:

- (1) Flow reversal upstream of the pier and downstream of the pier, flow wake occurs,
- (2) (DS-FRNP) minimizes the turbulent kinetic energy at the upstream face of the pier as compared with circular and (US-FRNP) respectively. This reduction of TKE indicates that the vorticity magnitude is more reduced for downstream-facing round-nosed pier, which results in reduced local scour.

## References

- Afzal, S. (2013). 3D Numerical Modeling of Sediment Transport under Current and Waves, Thesis presented to the Norwegian University of Science and Technology, in partial fulfillment of the requirements for the degree of Master of Engineering.
- Graf, W., & Istarato, I. (2002). Flow pattern in the scour hole around a cylinder. *Journal of Hydraulic Research*, 40(1), 13-20.
- Guemou, B. (2013). Numerical investigations of the bridge pier shape influence on the bed shear. Academic Center of Ain Temouchent, Algeria, vol. 18, Bund. Y. 5686.
- Mammar, M., & Soudani, A. (2012). Numerical study of external turbulent flow. *Revue des Energies Renouvelables*, 15, 155 – 164
- Nagata, N., Hosoda, T., Nakato, T., & Muramoto, Y. (2005). Three-dimensional numerical model for flow and bed deformation around river hydraulic structures. *Journal of Hydraulic Engineering, ASCE*, 131(12), 1074-1087.
- Oliveto, G., & Hager, W.H. (2002). Temporal evolution of clear-water pier and abutment scour. *Journal of Hydraulic Engineering, ASCE*, 128(9), 811-820.
- Roulund, A., Sumer, B. M., Fredsoe, J., & Michelsen, J. (2005). Numerical and experimental investigation of flow and scour around a circular pile. *Journal of Fluid Mechanics*, 534, 351–401.
- Tseng, M. H., Yen, C.L., & Song, C.S. (2000). Computation of three-dimensional flow around square and circular piers. *International Journal for Numerical Method in Fluid*, 34, 207-227.
- Wilcox, D. C. (1994). *Turbulence Modeling for CFD*. DCW Industries Inc., La Canada, California.